Borys VINOGRADOV[1]

MECHANICAL SYSTEMS WITH AIR SPRING FLEXIBLE ELEMENTS

Summary. The purpose of this study was to assess the effectiveness of flexible air-spring systems operating in parallel to share the total load, taking into account installation and in-operation errors. This study presented experimental and calculated characteristics of the air spring flexibility and its dependence on the polytropic index and additional volume. It considered patterns of load distribution between the air springs when they are operating in parallel to share the total load for the case when the air springs were used as the supporting elements for various machines and units, and between transmission lines containing flexible couplings, where air springs were installed as flexible elements.

Keywords: air spring, rubber-cord shell, load distribution, flexible

1. INTRODUCTION

A wide standard size series of rubber-cord air springs with a load capacity from 350 N to 230,103 Nwas developed and is being produced. Prospects for effective use of air springs as hydraulic inertial transducers of motion [1], vibration dampers and shock absorbers for rail vehicles [2] are being considered. The use of pneumatic couplings in machine drives solved the problem of limiting dynamic loads [3, 7]. One of the most important features of pneumatic couplings is the ability to control their stiffness and, accordingly, torsional vibrations of

---

[1] Faculty of Mechanical, Ukrainian State University of Chemical Technology, Gagarin 5 Street, 49005, Dnepro, Ukraine. Email: borvvin@gmail.com

mechanical systems [4]. Furthermore, air springs may be effectively used as flexible elements sharing the total load, and in systems with a branched power flow.

2. FLEXIBILITY CHARACTERISTICS OF AIR SPRINGS

When choosing a reference point in the static equilibrium position, the characteristics of the air spring flexibility has the form

$$F(x) = S(x)\left[(p_{at} + p_{m0})\frac{V_{G0}}{V_{G0} - \int_0^x (x)\,dx} - p_{at}\right] \tag{1}$$

where V_{G0}, p_{m0} are the gas volume and overpressure in the air spring bellows in the static equilibrium position; p_{at} is atmospheric pressure; S_x is the air spring effective area depending on the displacement x.

The experimental studies of the flexibility characteristics were carried out for the Connect MD 1895 double convolution air spring, according to the manufacturer's company catalogue, its features are: weight - 2.95 kg; working pressure - 0.5 MPa; maximum pressure - 0.8 MPa; minimum pressure - 0 MPa; working diameter - 265 mm; assembly height 210 mm; load capacity - 900 kg. The internal volume of the air spring with its design height of 140 mm is 3.64 litres. Based on experimental studies, the dependence of the air spring effective area on its deformation is represented by a first-order polynomial.

$$S(x) = S_0 + \beta x, \tag{2}$$

where $S_0 = \dfrac{P}{p_{mo}}$ is the effective area in the static equilibrium position, m², P is the external load, $\beta = 0.118$ m.

The difference between the experimental and calculated flexibility of the air spring, when compared by the formula (1) given (2), does not exceed 2%, which allows for further consideration of it as an actual flexibility [5].

Expanding the expression (1) considering (2) in a Taylor series and retaining only the first two terms, we obtain

$$F_1 = F_{10} + cx, \tag{3}$$

where

$$F_{10} = p_{m0} S_0,$$

$$c = \beta p_{m0} + \frac{n S_0^2 (p_{at} + p_{m0})}{V_{G0}} \tag{4}$$

Figure 1 shows the linearised flexibility characteristics, determined by the formula (4), with the actual flexibility determined by the formula (1)

The rubber-cord flexible element is a closed system, where heat will be evolved due to internal air friction during each cycle of air compression and expansion. The value of the polytropic index depends on the conditions of heat removal. The environmental conditions being the same, the number of compression and expansion cycles over the same time period grows with an increase in the vibration frequency; with the lack of proper heat removal, the polytropic index can take values $n > 1.4$. In most cases, the calculations take $n = 1.3$. As n increases, for example, from 1.3 to 1.6, as it follows from expression (4), the air spring

stiffness and the natural frequency increase by 1.13 (Figure 2a) and 1.06 times, respectively, which in practice can be neglected in most cases.
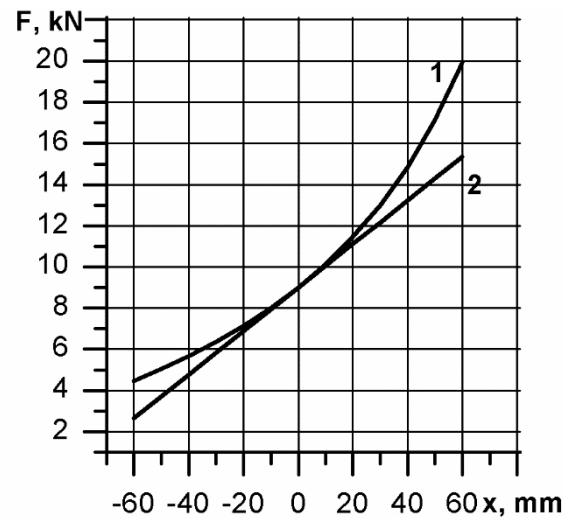
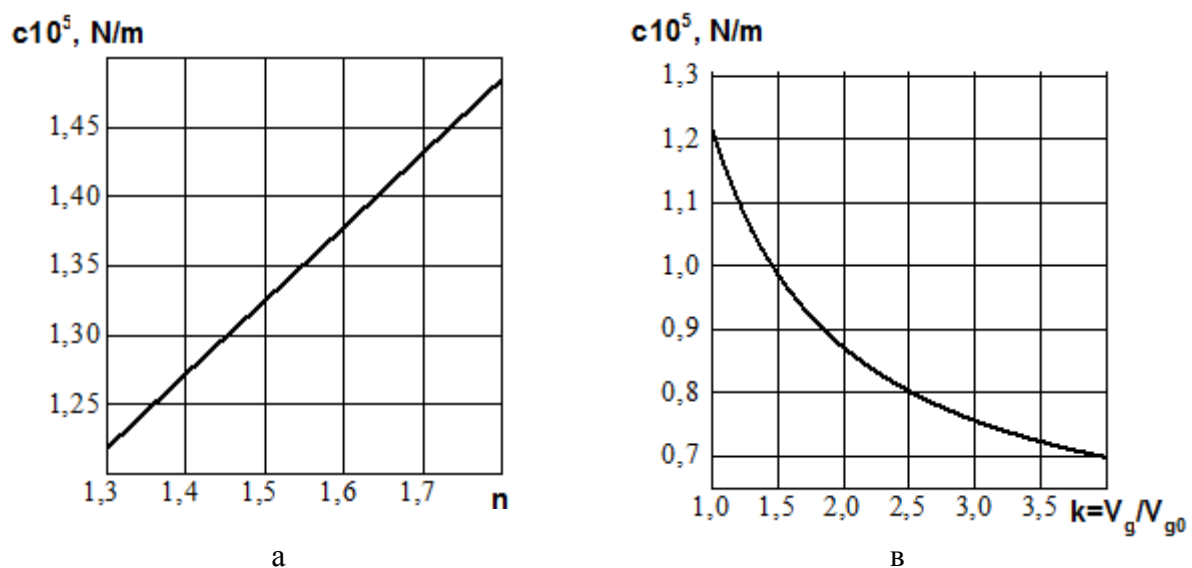Fig. 1. Actual and linearised flexibility characteristics of the air spring

Fig. 2. The dependence of the air spring stiffness on the polytropic index (a) and the additional volume (b): k is the ratio of the total volume of gas (including the added gas) to the initial volume

The rubber-cord flexible element is a closed system, where heat will be evolved due to internal air friction during each cycle of air compression and expansion. The value of the polytropic index depends on the conditions of heat removal. The environmental conditions being the same, the number of compression and expansion cycles over the same time period grows with an increase in the vibration frequency; with the lack of proper heat removal, the polytropic index can take values n > 1.4. In most cases, the calculations take n = 1.3. As n increases, for example, from 1.3 to 1.6, as it follows from expression (4), the air spring stiffness and the natural frequency increase by 1.13 (Figure 2a) and 1.06 times, respectively, which in practice can be neglected in most cases.

One of the advantages of systems that use air springs as flexible elements is the ability to control their flexibility by adding an additional volume (Fig. 2b)

3. LOAD DISTRIBUTION BETWEEN AIR SPRINGS OPERATED IN PARALLEL TO SHARE THE TOTAL LOAD

Consider the case where air springs are used as support for various machines and units. These mechanical systems include vibratory machines or other aggregates that apply air springs as flexible elements. This is the case, where installation errors may occur when the support of one air spring is displaced by Δ relative to the other (Fig. 3).

When pressure is supplied to the bellows of each air spring, the error is compensated and the air springs will attain equal pressures. Interconnected air springs adjust the pressure automatically. In the state of static equilibrium position, the first air spring will undergo a deformation smaller by the value of Δ. As a result, the effective areas of the air springs in the static equilibrium position will be different; pressures p_{m0} being the same, the load between the air springs will not be uniformly distributed.
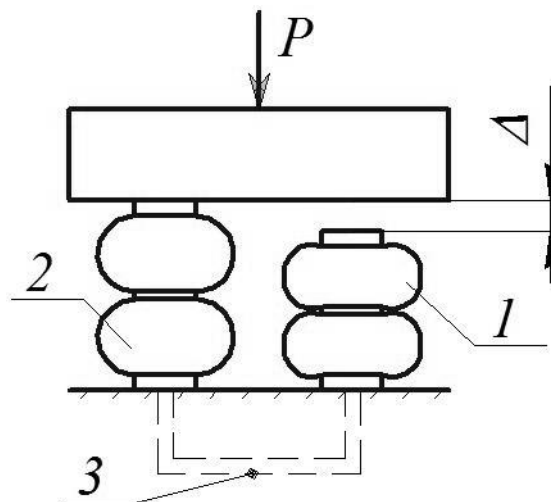

Fig. 3. Flexible system with air springs mounted in parallel: 1, 2 - air springs; 3 - common pipeline; P - external load; Δ - the error

For the case of independent operation of air springs, the equilibrium equations will take the form:

$$F_1 = S(x_1)p_1, \quad F_2 = S(x_2)p_2, \quad F_1 + F_2 = P,$$

where $x_1 = x - \Delta x$, $x_2 = x$

Substituting $S(x_1)$, $S(x_2)$, p_1, p_2 from (1), we obtain the system of equations

$$F_1 = [S_0 + \beta(x - \Delta)]\left\{(p_{at} + p_{u0})\left[\frac{V_{G0}}{V_{G0} - \int_0^x [S_0 + \beta(x-\Delta)]dx}\right]^n - p_{at}\right\}, \qquad (5)$$

$$F_2 = (S_0 + \beta x)\left\{((p_{at} + p_{m0}))\left[\frac{V_{G0}}{V_{G0} - \int_0^x (S_0 + \beta x)\ dx}\right]^n - p_{at}\right\}, \qquad (6)$$

The value of x in the static equilibrium position is determined from the following condition:

$$[S_0 + \beta(x - \Delta)]\left\{\left[(p_{at} + p_{m0})\frac{V_{Go}}{V_{GO} - \int_0^x [S_0 + \beta(x - \Delta)]dx}\right]^n - p_{at}\right\} +$$

$$+(S_0 + \beta x)\left\{((p_{at} + p_{m0}))\left[\frac{V_{Go}}{V_{Go} - \int_0^x (S_0 + \beta x)dx}\right]^n - p_{at}\right\}.$$

When linearising the flexibility characteristics, the stiffness of the air springs is determined by the following expressions

$$c_1 = \beta p_{m0} + \frac{(S_0 - \beta\Delta)^2 n(p_{at} + p_{m0})}{V_{Go}},$$

(7)

$$c_2 = \beta p_{m0} + \frac{S_0^2 n(p_{at} + p_{m0})}{V_{GO}}$$

The calculated values of the linearised air spring stiffnesses versus the magnitude of the error Δ are shown in Figure 4.
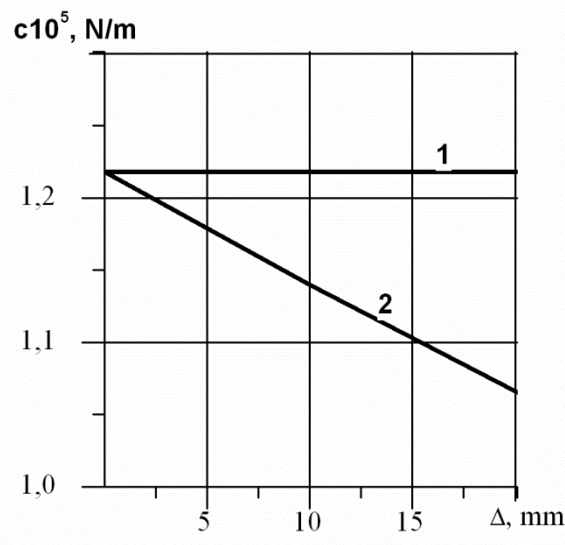

Fig. 4. Dependence of the air spring stiffness on the error Δ for independent air springs, the initial pressures p_{m0} being equal

The calculated data showed that the mounting errors, in this case, have little effect on the change in stiffness. Even with an error of 20 mm, the stiffnesses of the air springs differ by no more than 1.2 times.

In the static equilibrium position, the air springs will take the force

$$F_1 = P\frac{c_1}{c_1 + c_2}, \qquad F_2 = P\frac{c_2}{c_1 + c_2}$$

(8)

The non-uniform distribution of the load will be characterised by the coefficient kN, which shows how many times the force taken by the most loaded air spring exceeds the force taken under a uniform distribution of the total load

$$k_N = \frac{F_{max}}{0.5P} \qquad (9)$$

Considering that $c_2 > c_1$, $F_{max} = F_2$, we obtain

$$k_N = 2\frac{c_2}{c_1+c_2}. \qquad (10)$$

When $c_1 = c_2 \qquad k_N = 1.$

The dependence of the non-uniform load distribution factor k_N on the magnitude of the error Δ is shown in Figure 5.
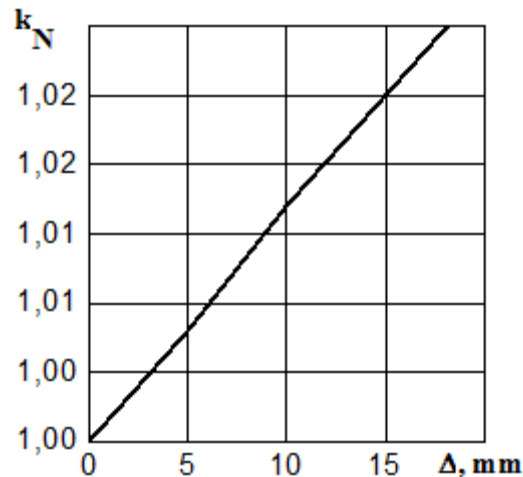

Fig. 5. The dependence of the non-uniformity factor k_N on the error Δ, the initial pressures p_{io} being equal

As can be seen from the expression (11) and (14), in this case, the non-uniform load was only caused by a change in the effective area, which, in turn, is caused by the mounting error.

Analyzing the data obtained, we can conclude that the use of air springs as flexible elements operating in parallel ensures a practically uniform distribution of the load between them. Even with an error $\Delta = 20$ mm, the non-uniform distribution of load is about 3%.

4. LOAD DISTRIBUTION BETWEEN TRANSMISSION LINES INCORPORATING PNEUMATIC FLEXIBLE COUPLINGS

As an example, we considered a twin-motor synchronous drive, whose transmission lines incorporate couplings with air springs installed as flexible elements (Fig. 6). Figure 1 shows a flexible coupling (pneumatic coupling) developed by the Polish company, FENA, at the Technical University in Košice (Slovakia) [5].

The feature of the synchronous drive is that the rotational speed of the motors does not depend on the load. At the moment, when the motors come into synchronism, their rotors may undergo angular displacement in respect to each other; this leads to an error, which we will further call an "angular mismatch". By the angular mismatch$\Delta\varphi$, we understood the angle by which it is necessary to align the rotors of the engine in order to provide a uniform load

distribution. Misalignment of the rotors may also be caused by the take-up of clearances in the kinematic chain.

The force taken by each air spring is determined by the following expressions:

$$F_1 = [S_0 + \beta(x - \Delta)]\left\{(p_{at} + p_{m0})\left[\frac{V_{G0}}{V_{G0} - \int_0^{x-\Delta}[S_0 + \beta(x - \Delta)]dx}\right]^n - p_{at}\right\}, \qquad (11)$$

$$F_2 = (S_0 + \beta x)\left\{((p_{at} + p_{m0}))\left[\frac{V_{G0}}{V_{G0} - \int_0^x(S_0 + \beta x)\ dx}\right]^n - p_{at}\right\}, \qquad (12)$$

$$[S_0 + \beta(x - \Delta)]\left\{(p_{at} + p_{m0})\left[\frac{V_{G0}}{V_{G0} - \int_0^{x-\Delta}[S_0 + \beta(x - \Delta)]dx}\right]^n - p_{at}\right\} +$$

$$+[S_0 + \beta(x - \Delta)]\left\{(p_{at} + p_{m0})\left[\frac{V_{G0}}{V_{G0} - \int_0^{x-\Delta}[S_0 + \beta(x - \Delta)]dx}\right]^n - p_{at}\right\} = P. \qquad (13)$$
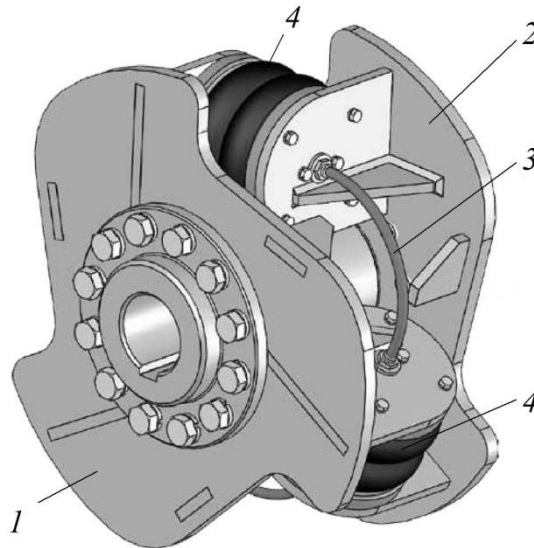

Fig. 6. Flexible pneumatic coupling:
1 - drive part; 2 - driven part; 3 - pipeline; 4 - pneumatic flexible elements
(rubber-cord air springs)

The variation of the non-uniformity factor versus the error for this case is shown in Figure 7.

In the case, when the bellows of the air springs of each coupling are interconnected, the mismatch of the motor rotors will be compensated by stretching the air spring bellows in the coupling of the first motor transmission line and compressing the air spring bellows in the coupling of the other motor transmission line, the pressure within the air springs being the same [6].

As a result, the non-uniform load distribution between the motors will only be due to the different effective areas of the air springs in the couplings; it can be determined by the formula (10). With a relatively high error $\Delta = 20$mm, the non-uniform load distribution will be about 3% (Figure 7). An absolutely uniform load distribution can be achieved by using an automatic system that enables control of the pressure within the bellows of the air springs [6].
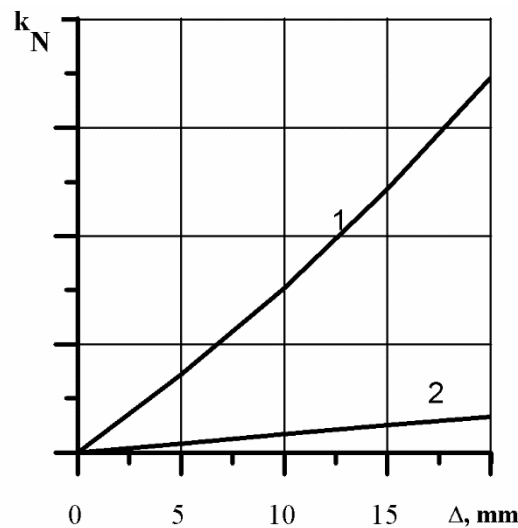
Fig. 7. The load distribution factor versus the magnitude of the angular mismatch of the synchronous motor rotors $\Delta = r\Delta\varphi_0$, ($r$ is the coupling radius): 1, 2 - couplings with independent and interconnected air springs, respectively

5. CONCLUSIONS

1. In the operation of pneumatic systems, the polytropic index n will change depending on the conditions of the heat removal. With an increase in n, for example, from 1.3 to 1.6, the air spring stiffness will increase by 1.13 and the natural frequency by 1.06 times, which in most cases can be neglected in practice.
2. In cases, when the air springs are mounted in parallel to support the total load, the load will be almost uniformly distributed between the air springs, even with equal initial air pressures in their bellows, and in spite of the relatively bad mounting errors (20 mm).
3. The use of flexible couplings in mechanical systems with branched power flows, for example, in twin-motor synchronous drives where air springs are used as flexible elements, allows an even distribution of the load between the transmission lines.

References

1. Buryan Yu.A., V.N. Sorokin, M.V. Silkov, Yu.F. Galuza. 2015. "Hydraulic inertial motion transformer with rubber-cord casing". *Omsk Scientific Bulletin* 1(137): 30-33.
2. Manashkin L., S. Myamlin, V. Prikhodkою 2009. *Oscillation dampers and shock absorbers in railway vehicles (mathematical models)*. Dnipropetrovsk. 180 p. DOI: 10.15802/978-966-348-121-0.
3. Czech P. 2012. „Determination of the course of pressure in an internal combustion engine cylinder with the use of vibration effects and radial basis function - preliminary research". *Communications in Computer and Information Science* 329: 175-182. 12th International Conference on Transport Systems Telematics (TST 2012). Katowice-Ustron, Poland, October 10-13, 2012. Telematics In The Transport Environment. DOI: https://doi.org/10.1007/978-3-642-34050-5_21.

4. Sága M., L. Jakubovičová. 2014. "Computational analysis of contact stress distribution in the case of mutual stewing of roller bearing rings". *Novel Trends in Production Devices and Systems, Applied Mechanics and Materials* 474: 363-368.
5. Sapietova A., V. Dekys. 2016. „Use od Msc. Adams software product in modeling vibration sources". *Komunikacie* 1a(101): 101-107.
6. Urbanský M., J. Homišin, P. Kaššay, J. Krajňák. 2018. „Measurement of air springs volume using indirect method in the design of selected pneumatic devices". *Acta Mechanica et Automatica* 12(1): 19-22. ISSN 1898-4088.
7. Żółtowski B., M. Żółtowski. 2018. "Selection measure of energy propagation in vibration diagnostic and modal analysis methods". *Diagnostyka* 19(4):19-26.
    DOI: 10.29354/diag/94753.